Actively mode-locked THz p-Ge hot-hole lasers with electric pulse-separation control and gain control

R. C. Strijbos,[a] A. V. Muravjov,[a] S. H. Withers,[a] S. G. Pavlov,[b] V. N. Shastin,[b] and R. E. Peale[a]

[a] Department of Physics, University of Central Florida, Orlando, FL 32816 USA

[b] Institute for Physics of Microstructures, Russian Academy of Sciences, GSP-105, Nizhny Novgorod 603600 Russia

ABSTRACT

Electric control of the separation between two interleaved pulse trains from a far-infrared (1.5-4 THz) p-Ge laser, which is actively mode-locked by rf gain modulation at the second harmonic of the roundtrip frequency, is demonstrated by changing the electric bias at the rf contacts. A suggested application is telemetry using pulse-separation modulation. Optimal operation of the laser on the light-to-heavy-hole transition requires strong, perfectly crossed electric and magnetic fields, but the experimental data reveal a electric-field component along the magnetic field caused by space-charge effects inside the laser crystal, even when the applied fields are perfectly orthogonal. Monte Carlo simulations together with a Poisson solver are used to discuss the various mechanisms behind these effects and to find the electric field inside the laser crystal. These calculations agree reasonably well with experimental data obtained so far, and show not only the significant impact that charging can have on the output of actively mode-locked p-Ge lasers, but also suggest that they strongly influence the average gain of p-Ge lasers in general.

Keywords: far-infrared, THz radiation, semiconductor lasers, active mode locking, hot hole transport, space charge, p-germanium

1. INTRODUCTION

To date p-Ge hot hole lasers are still the only solid-state lasers in the far-infrared region ($50-140$ cm^{-1} or $1.5-4$ THz). In contrast to conventional semiconductor lasers, where the lasing transition is between the conduction and valence band, here lasing occurs between different valence subbands, and p-Ge lasers can therefore be classified as unipolar or intersubband semiconductor lasers. Population inversion occurs in a bulk laser rod of relatively lightly doped p-type germanium $N_A \approx 10^{14}$ cm^{-3}) at helium temperatures ($T \lesssim 20$ K) and is based on the largely different motion of light and heavy hot holes in strong crossed electric and magnetic fields ($E \approx 0.3-3$ kV/cm, $B = 0.3-3$ T). The laser is usually operated at a 1-10 Hz repetition rate, and delivers microsecond pulses of a few Watt peak power. The laser can be tuned in the whole range from $1.5-4$ THz,[1] and considerable progress has been made towards developing a continuous-wave (CW) laser for use as a local oscillator for far-infrared heterodyne spectroscopy.[2] On the other hand, the broadband nature of the light-to-heavy hole band laser opens the possibility to generate picosecond, high-intensity pulses in the far infrared, a desirable feature for time-resolved (linear and non-linear) THz spectroscopy and other related applications, that is currently only available using free-electron lasers. Recently, active mode locking has been unambiguously demonstrated[3–5] in the time domain, resulting in a train of FIR pulses of about 200 ps. In this contribution, our recent results on mode-locked p-Ge lasers will be presented. Harmonic mode locking is demonstrated, and the delay between the two pulses traveling in the cavity can be electrically tuned from zero to half the cavity roundtrip time. Clear experimental evidence is found for the occurrence of space charge in the laser crystal. To account for the observed phenomena, a detailed understanding of the hot hole transport underlying p-Ge lasers is necessary. Therefore, the basic features of hot hole transport in crossed fields and the pumping mechanism of p-Ge lasers are first shortly recapitulated in section 1.1 using a simple isotropic model.

1.1. Hot hole transport in crossed fields and pumping mechanism

A relatively low impurity concentration and liquid helium temperatures are required to obtain lasing in p-Ge crystals. In these conditions the emission of an optical phonon is by far the most probable scattering process (i.e. $\tau_{op} \sim 0.1$ ps), but it requires

Part of the SPIE Conference on Terahertz Spectroscopy and Applications
San Jose, California • January 1999 SPIE Vol. 3617 • 0277-786X/99/$10.00

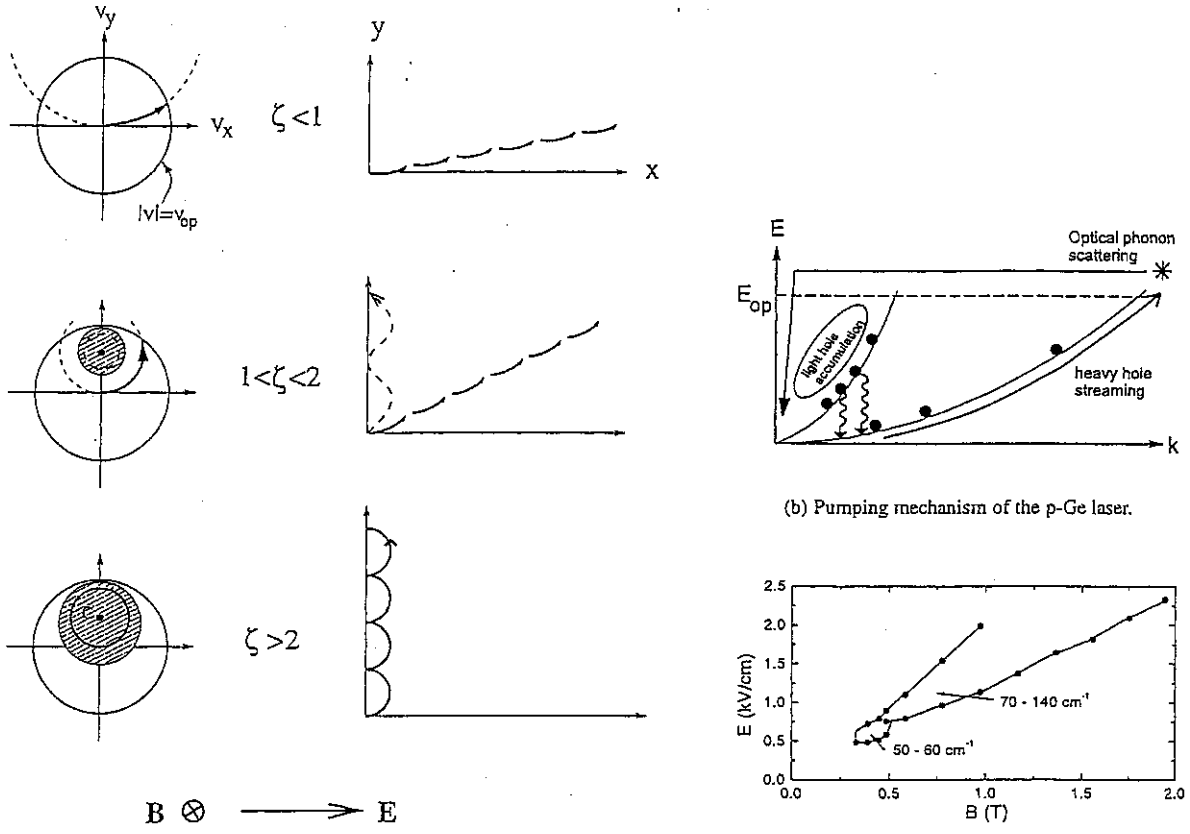

(a) Illustration of the typical hole orbits in crossed E and B fields in velocity space (left) and real space (right) as a function of the parameter ζ.

(b) Pumping mechanism of the p-Ge laser.

(c) Typical (E,B) field regions for a p-Ge laser.

Figure 1. Basics of p-Ge lasers.

that the hole energy ε exceeds the optical phonon energy $E_{op} = 37$ meV. For $\varepsilon < E_{op}$ the scattering is due to acoustic phonons and ionized impurities only ($\tau_c \approx 10 - 100$ ps) and is strongly suppressed due to the low T and N_A, respectively.

The large distinction between scattering rates above and below the optical phonon energy permits an accurate description of hole transport using a simple isotropic band model. Possible hole orbits in crossed fields are shown in Fig. 1(a) both in velocity space (left) and in real space (right). Three different situations are discerned, labeled by the parameter $\zeta = v_{op}/v_D$, where $v_{op} = \sqrt{2E_{op}/m^*}$ (with m^* the hole effective mass) is the velocity corresponding to a kinetic energy equal to the optical phonon energy E_{op}, and $v_D = E/B$ is the center of the hole orbits in velocity space. For $\zeta < 1$ the holes are in so-called streaming motion. They are repeatedly accelerated up to the optical phonon energy E_{op} and scattered back to the Γ point by emitting an optical phonon. For $1 < \zeta < 2$ still most holes are streaming (with a larger Hall-angle α_H between the current j and E), but around the center point $C = (0, -v_D)$ cyclotron orbits appear that are closed within the optical phonon contour $v = v_{op}$. As holes on these orbits can no longer emit an optical phonon, they are trapped or accumulated on closed cyclotron orbits with lifetime τ_c. For $\zeta > 2$ also the principal orbit through the Γ point is closed within $v = v_{op}$ and basically all holes are within the accumulation region.

However, the valence band of germanium is degenerate at the Γ point and consists of a light and heavy hole subband with a large difference in effective mass ($m_l = 0.043m_0$ and $m_h = 0.35m_0$, respectively, with m_0 the mass of a free electron). The motion of light and heavy holes in crossed fields is, therefore, characterized by different values of the parameter ζ, and this

Correspondence: Email: rep@physics.ucf.edu; WWW: http://www.physics.ucf.edu/~rep; Telephone: 407-823-3076; Fax: 407-823-5112

forms the basis for the pumping mechanism of the light-to-heavy hole band laser as shown in Fig. 1(b). For properly chosen E and B values, all light holes are accumulated ($\zeta_l >> 2$), while heavy holes are (partially) in streaming motion ($\zeta_h < 2$). The upper laser level has, therefore, a much longer lifetime than the lower level. The latter is depopulated by heavy hole acceleration by the electric field, while the former is pumped by the 4% of the streaming heavy holes that end up in the light hole band after optical phonon emission. Therefore, all necessary conditions for establishing a laser on the light-to-heavy-hole transition (or Inter-Valence-(sub-)Band (IVB) transition) can be met. Fig. 1(c) shows the typical region of E and B fields, where lasing is observed experimentally, showing excellent agreement with the predictions of the above model.

1.2. gain modulation and mode locking

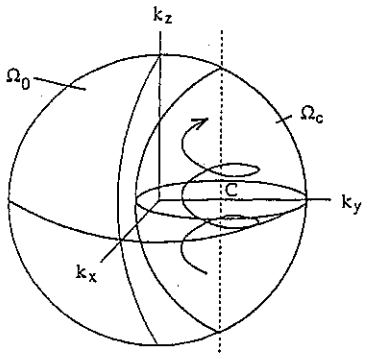

(a) Light holes spiraling in the accumulation region Ω_c beyond the optical phonon energy Ω_0 due to a small electric field E_L in the direction of the magnetic field.

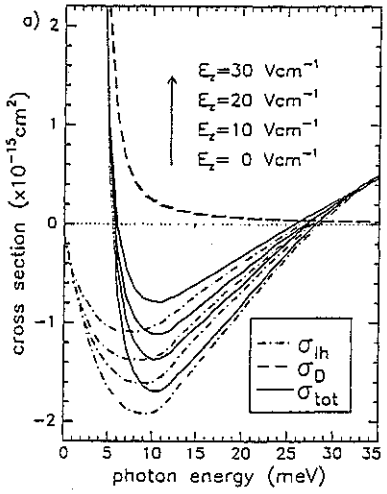

(b) Dependence of small-signal gain on E_L, $T = 10$ K, $E = 1.15$ kV/cm $\|< 1\bar{1}0 >$ $B = 0.9$ T $\|< 112 >$, $N_I = 1.2 \times 10^{14}$ cm^{-3}, $p_0 = 7 \times 10^{13}$ cm^{-3}, Brooks-Herring model with self-consistent screening.

Figure 2.

From Fig. 1(b) it is clear that the IVB p-Ge lasers can have a wide output spectrum (typically a width of 20-30cm^{-1}is observed) and are, therefore, very suitable for the amplification or generation of THz pulses on a picosecond timescale. The latter requires an element in the laser cavity whose gain or loss in the far infrared can be modulated. Such an element has to operate in cryogenic conditions, however, preferably in the whole frequency range of p-Ge laser emission. Moreover, inclusion of an external element in the laser cavity is expected to cause reflections at the interfaces that might complicate mode locking. To avoid such problems it was proposed in Ref. 6 to induce active mode locking by radio-frequency (rf) gain modulation at one end of the laser crystal. This is rather similar to a method used for active mode locking of semiconductor diode lasers, where the pump current is modulated by applying an rf field in addition to the constant bias. In our case, however, not the magnitude of the pump current is changed, but rather its direction. This is achieved by applying the rf to two small additional contacts perpendicular to the main high-voltage contacts of a Voigt-configured p-Ge laser, where the applied electric and magnetic field are perpendicular to the long axis of the laser crystal. The rf field thus introduces small electric field components E_L along the magnetic field, and it is easily understood why this decreases the small-signal gain significantly. As shown above (Fig. 1(a)), the magnetic field restricts the motion of accumulated light holes in the transverse plane such that their kinetic energy remains below the optical phonon energy. However, along the magnetic field they can still move freely with very high mobility, and a small E_L field will turn the closed cyclotron orbits of Fig. 1(a) into spiral-like orbits as shown in Fig. 2(a). Eventually the light holes are accelerated beyond the optical phonon energy, they emit an optical phonon, and are primarily scattered into the heavy hole band. Therefore, the population inversion and the small-signal gain decrease. Clearly, this method is only effective when

the E_L field accelerates the light holes beyond E_{op} before they are scattered back to the heavy hole band anyway by interband scattering on acoustic phonons and ionized impurities.

Monte Carlo simulations show that for the usual temperatures and ionized impurity concentration, the desired effect is easily accomplished, and a small rf electric field (only a few percent of the main pumping electric field) along the magnetic field is already enough to modulate the gain by 30-50% (see Fig. 2(b)). When the gain is modulated at (a harmonic of) the roundtrip frequency, only the pulse traveling through the modulator at maximum gain is continually amplified, yielding the typical pulse-train output of an actively mode-locked laser.

2. EXPERIMENTAL SETUP

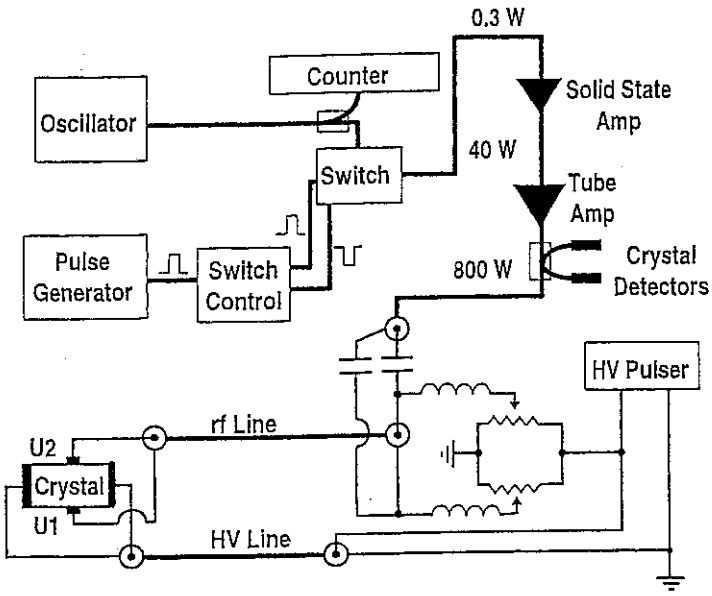

(a) Rf setup. Thick lines denote coaxial lines.

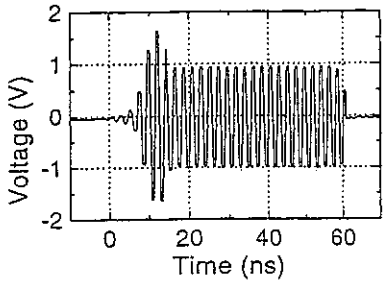

(b) (Attenuated) output of the pulse-forming switch

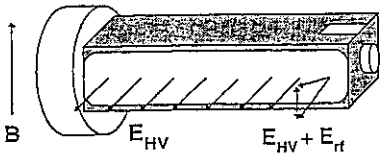

(c) The p-Ge laser crystal with applied fields and mirrors

Figure 3.

Single-crystal, Ga-doped, p-Ge ($N_D - N_A = 7 \times 10^{13}$ cm^{-3}) is cut into rectangular bars with a cross section of 7×5 mm^2. Crystal lengths are chosen 42.1 and 84.2 mm such that the laser roundtrip frequencies match the rf frequency ν_{rf} near 452 MHz of relatively cheap ham-radio electronics or its second harmonic. The two opposite lateral $5 \times L$ mm^2 sides of the crystal are evaporated with aluminium and subsequently annealed to provide Ohmic contacts for the main high-voltage (HV) field. At the same time, small additional contacts with a length of ~ 4 mm are fabricated at one end of the crystal perpendicular to the main contacts (Fig. 3(c)). Applying a constant bias or an rf field to these contacts introduces a local, small, additional electric field $E_L \parallel B$, which is used to modify or modulate the small-signal gain at one end of the laser crystal. The crystal ends are polished parallel to each other within 1' accuracy and two external copper mirrors (with diameters of 7 and 5 mm) are attached to them via a 20 μm thick teflon film to form an external resonator (Fig. 3(c)). The p-Ge crystals are immersed in liquid helium at 4.2 K in a cryostat (Janis 8DT), and placed between the poles of a room temperature electromagnet (Walker Scientific HF-9H), which provides magnetic fields up to 1.4 T in Voigt geometry (i.e. the magnetic field is perpendicular to axis of the laser resonator). Electric field pulses E_{HV} are applied from a low duty-cycle thyratron pulser. The field orientations are $E_{HV} \parallel [1\bar{1}0]$ and $B \parallel [112]$. Radiation emitted from around the smaller outcoupling mirror is collected and conducted out of the top of the cryostat using a brass light pipe. A teflon lens was used to seal the light pipe and focus the laser output radiation on a whisker-contacted Schottky-diode detector, biased using a simple homemade battery-powered current source and a Minicircuits 15542 bias-T. The diode chip (1T17(82)) was purchased from the University of Virginia and the corner cube was made by Savant-Vincent, Inc.,

Tampa, FL. Whiskers were formed, electrolytically sharpened, and contacted to the diode by the authors. The detector signal is boosted by a Picosecond Pulse Labs 5840 amplifier with 10 GHz bandwidth, and recorded on a Tektronix SCD5000 transient digitizer with 4.5 GHz analog bandwidth, 200 G-samples/s, and 11 bits vertical resolution (2 mV quantization steps).

Fig. 3(a) shows the rf system assembled for the experiments to produce clean sub-μs pulses which just overlap the HV pulses to prevent heating of the laser crystal by the rf. Since the impedance of the crystal between the rf contacts is low, high rf power is required, in part to overcome the unavoidable imperfect impedance match to the dynamic load. The General Radio 1362 UHF oscillator delivers about 0.3 W CW signal that is frequency stable within a few tens of kHz. A directional coupler feeds a fraction of this signal to a Stanford Model SR620 frequency counter. The main part goes to a Minicircuits Model 15542 PIN diode switch controlled by 8 V signals from a home built controller, that itself is driven by standard TTL pulses. The (attenuated) signal after the switch is plotted in Fig. 3(b) and demonstrates the sharp rise and fall and the short pulse lengths obtainable. From the switch, low duty-cycle rf bursts enter a GE MASTR II solid-state power amplifier with gain control to give up to 40 W. This is fed to a Henry Radio Model 2004A tube amplifier to give up to 800 W. A Microwave Devices 318N3 directional coupler and HP 420A crystal detectors monitor forward and reflected rf power. Power measurements were verified by direct observation of the rf voltage on a fast oscilloscope. Simple isolation capacitors were used to improve impedance match to the dynamic load and protect HV and rf systems from each other. Additionally, a bias $U_2 - U_1$ can be supplied to the small contacts from the main high voltage pulse by setting the potentials U_1 and U_2 using two variable voltage dividers. This is a new feature compared to the set-ups described in Refs. 3,4 and turns out to be a very important parameter for controlling the output of the mode-locked p-Ge laser, as will be described in the next section.

3. RESULTS AND DISCUSSION

3.1. Active mode locking

3.1.1. 42.1 mm sample

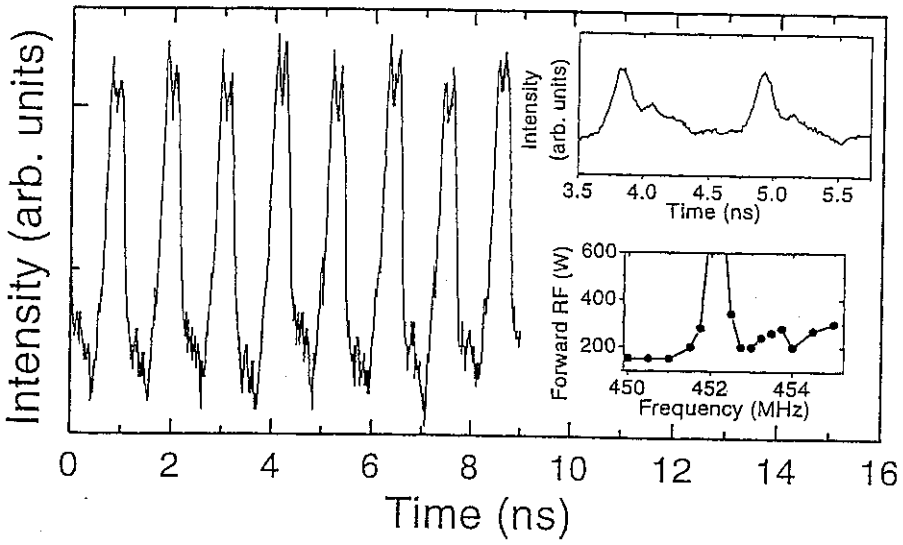

Figure 4. Output from the actively mode-locked 42.1 mm laser crystal. The upper inset shows a different shot with 150 ps pulses. In the lower inset the rf resonance at half the roundtrip frequency is plotted.

A summary of our first mode-lock results for the 42.1 mm sample upon applying rf during the laser pulse is given in Fig. 4. For arbitrary rf frequencies the E_L field due to the rf reduces the gain in the region between the additional contacts and the laser can be brought below threshold by increasing the rf power. The forward rf power required to extinguish lasing is plotted in the lower inset of Fig. 4 versus the rf frequency. At 452.2 MHz a resonance occurs, where the laser still operates even when the full available forward rf power is applied. This frequency corresponds to half the cavity roundtrip frequency. However, since we expect the gain to be maximal at the rf nodes ($E_L = 0$) and minimal at the rf extrema, and hence the gain to be modulated at twice the rf frequency, the condition for active mode locking that the gain is modulated at the roundtrip frequency is met.

Shifting the modulation frequency by more than ±0.5 MHz blocks the lasing, as expected for a mode-locked laser because circulating pulses do not remain in phase with the gain modulation. At resonance, the Schottky diode detector signal registers the mode-locked pulse train plotted in Fig. 4. The upper inset shows 150 ps pulses from a different shot. The basic pattern of pronounced, separated pulses is repeatable with only minor differences from shot to shot.

It is noted here that for the experiment of Fig. 4, a bias of about 20 V is applied to the rf contacts in addition to the rf power. Changing this bias by more than about 5 V removes the resonance observed in Fig. 4. This indicates that for this particular situation mode locking is only possible with the bias. The implications of this will be discussed in section 3.2 together with additional measurements.

3.1.2. 84.2 mm sample

a)

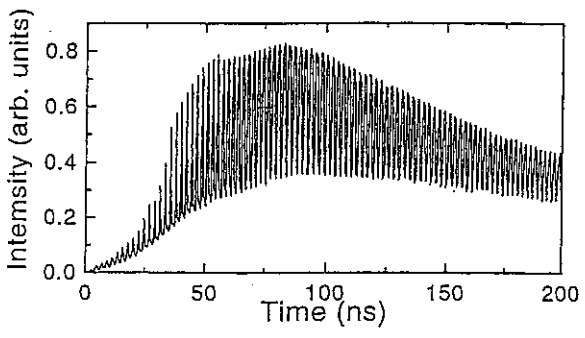

(a) Output of the actively mode-locked 84.2 mm long laser crystal.

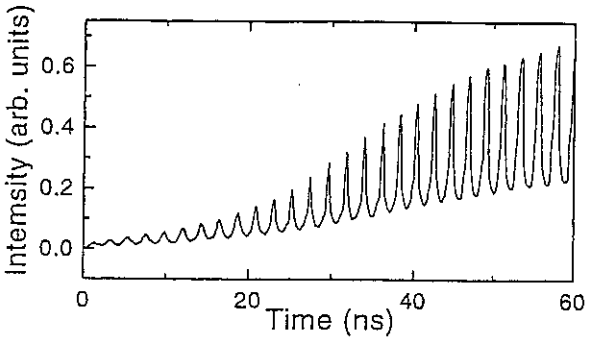

(b) The development of a pulse of increasing intensity and decreasing pulsewidth in the laser cavity is clearly reflected in the start of the pulse train.

Figure 5.

The experiments are repeated for a laser crystal that is twice as long as in the previous section. The length of $L = 84.2$ mm now corresponds to a roundtrip time $T = 2 * n_{Ge} L/c = 2.20$ ns, where $n_{Ge} = 3.925$ is the refractive index of germanium, and c is the speed of light, and the roundtrip frequency is $\nu_{RT} = 1/T = 453.6$ MHz. Again this is very close to the experimentally found resonance at 453.8 MHz, where the applied rf is unable to extinguish lasing even at maximum rf power, indicative of mode-locked behavior. Figure 5 shows the output pulse train of the actively mode-locked pulse train as detected on the Schottky diode and registered at the transient digitizer. The pulses are separated by the roundtrip time $T = 2.20$ ns, as it results from a single pulse traveling to and fro within the resonator and partially coupled out each time it hits the outcoupling mirror. A close-up of the start of the pulse train clearly shows the shortening of the pulse in the resonator as its intensity grows.

When the constant bias to the rf field is changed by changing the potentials U_1 and U_2 using the voltage dividers, again the output of the actively mode-locked laser changes drastically, as can be seen in the left part of Fig. 6, where the output pulse train is plotted for different settings of the external bias $(U_1 - U_2)$. At zero external bias, a train of pulses separated by the roundtrip time is observed, similar to the ones shown in Fig. 5. However, when the external bias is increased, the mode-locked pulses start to broaden and eventually split into two. A further increase of the bias causes further separation of the pulses, and the distance between these pulses can be tuned to approximately half the roundtrip time of the laser cavity.

This behavior is interpreted in the right part of Fig. 6, where the expected time dependence of the modulated gain is plotted based on the theoretically determined decrease of gain as a function of the E_L field along the magnetic field direction (see Fig. 2(b)), as shown in the upper left corner of each subfigure. In each of these figures, the rf signal shown in the lower left corner is biased at a different level, and the upper right curve shows the resultant modulation of the small-signal gain in time, while the lower right bold curve shows the expected output pulse train.

At a certain bias value (set by the voltage $U_1 - U_2$ in Fig. 3(a) between the additional contacts), the rf field is applied at the peak of the gain-versus-E_L curve [situation (C) in Fig. 6]. Hence gain modulation occurs at twice the rf frequency, and the double pulse output from harmonic mode locking is expected. Moving the bias away from the point of maximum gain, the gain

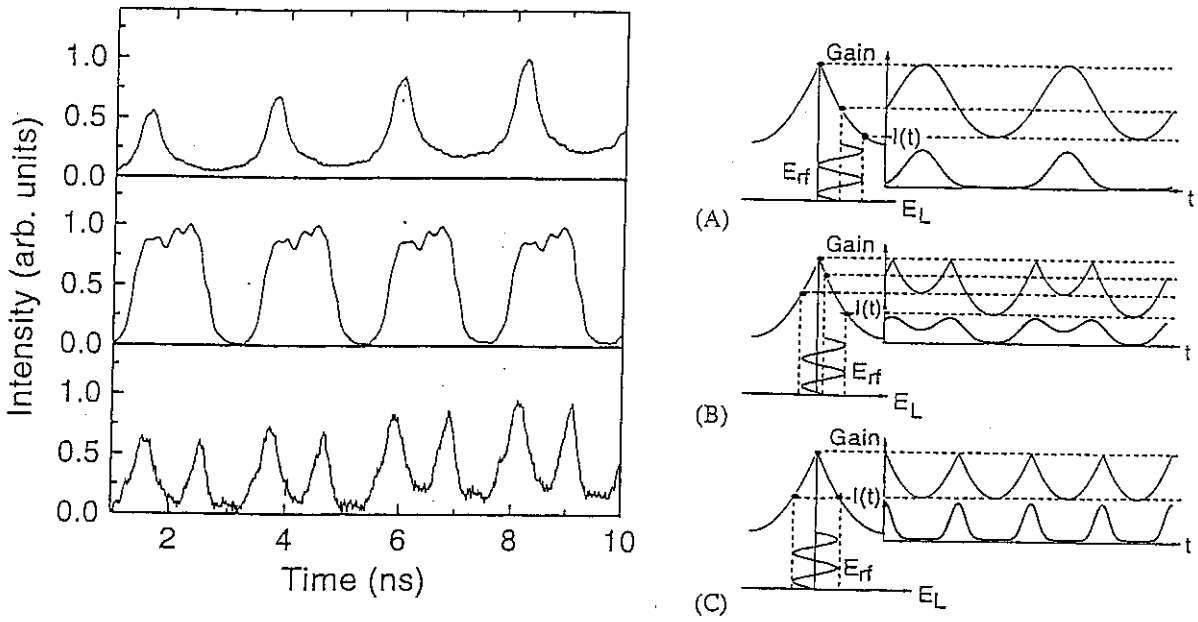

Figure 6. Experimentally observed pulse structure for the mode-locked 84.2 mm long p-Ge crystal (left) and theoretical model (right) for pulse-separation control. The three situations to the right mimic the experimental results to the left. They correspond to (A) large offset: modulation far from peak of gain-vs.-E_L, (B) small offset: modulation close to peak of gain-vs.-E_L curve, and (C) zero offset: modulation at peak of gain-vs.-E_L curve.

is more and more modulated at the single rf frequency, and the pulses in each pair move toward each-other [situation (B)], until they are completely merged and a train of single pulses is generated [situation (A)].

Although the model in Fig. 6 gives a satisfactory agreement with the experimental results, this is only achieved when the experimentally observed output without external biasing (single-pulse mode locking) is connected to a situation where the rf modulation is already offset from the top of the gain-vs.-E_L curve [situation (A)]. Apparently, external biasing is necessary to reduce the internal E_L field and bring the rf modulation closer to the top of this curve yielding the broadened and eventually split pulses that are characteristic for situations (B) and (C).

Note that a similar effect was observed for the 42.1 mm crystal: an external bias of about 20 V was required to obtain mode locking. Again, this is well understood in the above model, keeping in mind that in this case mode locking is only possible when the gain is modulated at twice the rf frequency, and the rf field should, therefore, be applied at the peak of the gain-vs.-E_L curve (situation (C)). A large offset (as in situation (A)) leads to gain modulation at the single rf frequency (or half the cavity roundtrip frequency). Then a pulse passing the modulator at maximum gain will experience the lowest gain (or a net loss) after one roundtrip, and mode locking will not occur. Even if rf powers are sufficient to pass through the gain maximum twice per rf cycle (situation (B)), the offset causes broadening of the micropulses and a decrease in their intensity since maximum gain occurs at moments other than the rf field zero crossings.

3.2. effects of space charge

In the previous sections it was shown that the active mode locking experiments for both the 42.1 mm and the 84.2 mm laser crystals suggest the existence of a small intrinsic electric field E_L in the region between the additional contacts, which necessitates external biasing to bring the zero level of the rf field to the top of the gain-vs.-E_L curve in order to achieve gain modulation at twice the rf frequency.

In a similar fashion it can be argued that this intrinsic E_L will decrease the small-signal gain for the normal, microsecond, pulsed operation of p-Ge lasers, and that external biasing could increase the gain in the region between the additional contacts to its maximum value at $E_L = 0$. To verify this, we have measured the range of potentials U_1 and U_2 at the additional contacts

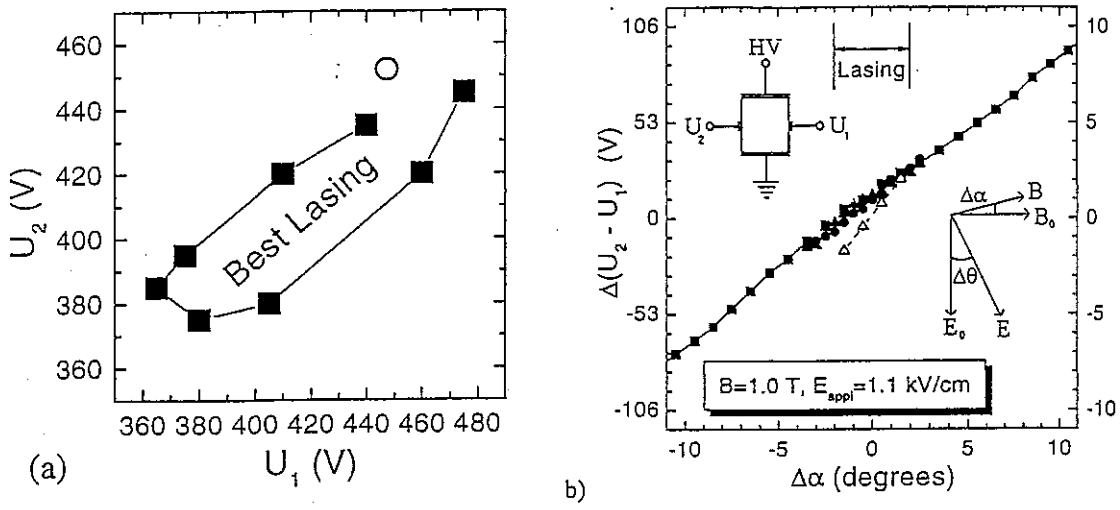

Figure 7. (a) Lasing domain in U_1, U_2 space. The open circle indicates the operating point without bias circuit. (b)Potential $U_2 - U_1$ on rf contacts when laser is rotated over an angle $\Delta\alpha$ around its long axis. Solid symbols denote the value without bias (different series indicate the error), while open triangles denote the external-bias setting with strongest lasing.

for which lasing is observed. The result is plotted in Fig. 7(a). The difference $U_2 - U_1$ might not be directly proportional to the E_L field in the region between the additional contacts, and $E_L = 0$ might not exactly occur for $U_2 = U_1$, as misalignment of the rf contacts might cause an offset. But the width of this region confirms the strong dependence of the gain on E_L: changing $U_2 - U_1$ over ± 50 V ($\Delta E_L \approx \pm 100$ V/cm) from its optimum value brings the laser below threshold. Moreover, it is found that the operating point without external bias (indicated by the open circle) lies on the border of this region and a voltage of about 15 V is necessary to move to the center of the lasing region with the highest small signal-gain. This value is in good agreement with the offsets previously found in the active mode-locking experiments.

Thus the experiments point to the existence of a intrinsic E_L field in the region between the additional contacts even when the applied fields are perfectly orthogonal to each other. It is important to note that this can only occur for situations with limited symmetry along the magnetic field, since for a perfectly symmetric situation E_L has to be zero by definition. And, indeed, the field orientation $E_{HV} \parallel [1\bar{1}0]$ and $B \parallel [112]$ used in our (and all previous[3–5,7,8]) active-mode-locking experiments lacks a symmetry plane perpendicular to the magnetic field in k-space. It has been argued before [9,10] that for such orientations a significant current $j_L \parallel B$ might occur even in perfectly crossed E and B fields. We suggest that this causes charging of our rectangular laser crystal at the sides perpendicular to the magnetic field (in a similar way as the usual Hall effect, i.e. to meet the boundary condition that the current flows parallel to crystal sides), which creates the E_L field observed.

Figure 8 presents the results of a Monte Carlo simulation for the component k_L of the average wavevector k along the B-direction (divided by the magnitude $k = |\mathrm{k}|$) and a similar quotient v_L/v for the average velocity vector, as a function of the magnetic field strength. The simulation is based on an anisotropic 'warped' band model, and simulates the hole motion in the experimental conditions.

Only the results for heavy holes are presented, since the contribution of light holes is comparatively small. The parameter ζ is also indicated to characterize the hole motion to one of the three situations in Fig. 1(a). Both k_L and j_L are non-zero for streaming holes ($\zeta < 1$), but increase drastically when holes start to accumulate ($\zeta = 1$) and reaches a maximum value just when the magnetic field is strong enough to trap most holes ($\zeta = 2$). Figure 9 gives a graphical illustration of this.[9,10] Figure 9(a) shows the strongly elongated hole distribution of streaming holes (schematically indicated by the bold contour lines) in the anisotropic band (the outer contour is the equi-energy surface $\varepsilon = E_{op}$) in the plane spanned by k_s and k_L, where k_s is the average wavevector of streaming holes. Because the velocity $v_n(\mathbf{k})$ (indicated by the arrow in Fig. 9(a)) is perpendicular to the equi-energy surface, a net positive velocity v_L will result (this is similar to well-known Sasaki-Shibuya effect[11] for streaming carriers in a strong electric field). For accumulated holes the accumulation region doesn't have the symmetric spindle shape of Fig 2(a), but has a much larger volume for $k_L < 0$ than for $k_L > 0$. This is shown in Fig. 9(b), where we have drawn the optical

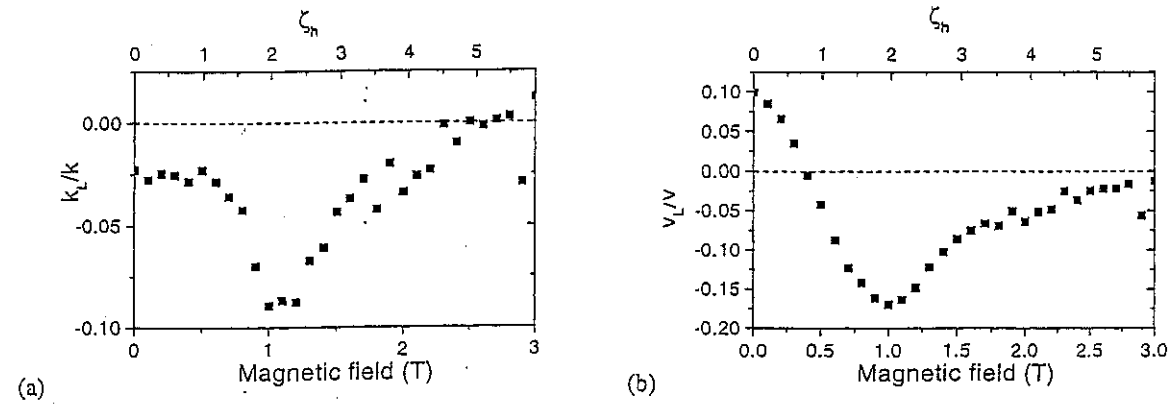

Figure 8. Simulated values of k_L/k and v_L/v as a function of magnetic field. $T = 20$ K, $E = 1.0$ kV/cm rotated over $\phi = 30°$ from $[1\bar{1}0]$, $B = 1.0\,\mathrm{T} \,||\, [112]$, $N_I = 1.3 \times 10^{14}\,\mathrm{cm}^{-3}$, $p_0 = 7 \times 10^{13}\,\mathrm{cm}^{-3}$, Brooks-Herring model with self-consistent screening.

phonon contour $\varepsilon = E_{op}$ (outer curve) and the border of the heavy hole accumulation curve (inner curve) in the planes $k_L > 0$ (solid curves) and $k_L < 0$ (dashed curves). Therefore, although all holes move on hole orbits perpendicular to the magnetic field, there are more holes with a $k_L < 0$ and therefore both the average k_L and current component j_L in the magnetic field direction have a non-zero, negative value

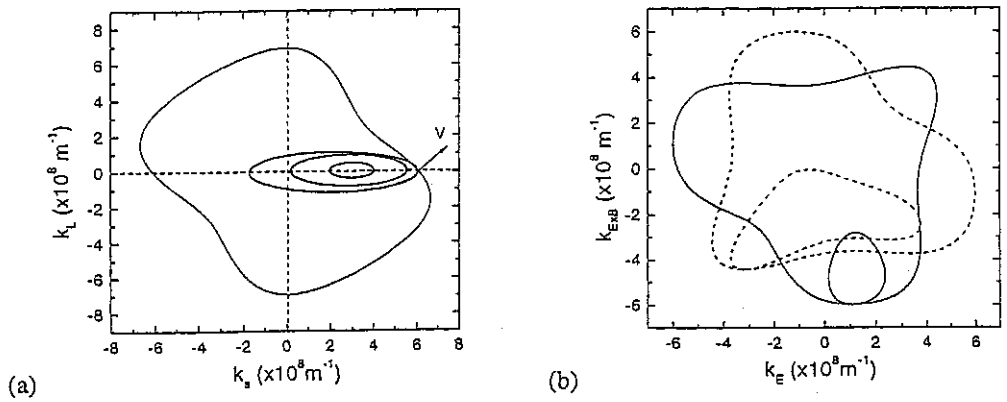

Figure 9. Explanation of the appearance of current component along the B-direction for $E_L = 0$ (so-called "Parallel Hall Effect"[9,10]): $E = 1.0$ kV/cm rotated over an angle ϕ from $[1\bar{1}0]$, $B = 1.0\,\mathrm{T} \,||\, [112]$ a) streaming hole distribution (bold contour lines) for $\phi = 30°$ in the k_x, k_L plane: b) accumulation region and optical phonon contour $\varepsilon = E_{op}$ for $k_L < 0$ (dashed lines) and $k_L > 0$ (solid lines), $\phi = 45°$

Although this basically provides the explanation for the offset, one more factor has to be taken into account, and that is the inhomogeneity of the electric field in a plane perpendicular to the magnetic field. Fig. 10(a) shows the calculated E-field in a cross-section of the 42-mm crystal perpendicular to B. Current saturation is implemented by taking the conductivity $\sigma_T \propto E^{-f}$, where f is the saturation parameter ($0 \leq f \leq 1$). Near the long ends, the total electric field $E_{tot} = (E_{HV}^2 + E_{Hall}^2)^{1/2}$ is larger and rotated over an angle ϕ with respect to E_{HV} due to the usual Hall effect. Space-charge effects significantly enlarge the affected area. This change of direction of the electric field has a strong impact on the magnitude of j_L, as shown in Fig. 10(b). Here, Monte Carlo[9] results for j_L (normalized by the total current j) are plotted when the E-field is rotated over an angle ϕ from the initial $[1\bar{1}0]$ due to the normal Hall effect. It is clear that, due to the inhomogeneity of E_{tot} caused by the normal Hall field, the E_L field is relatively small in the central part of the sample, but quite strong in the region between the additional contacts. When

the gain is optimized in central part of the laser crystal (by compensating E_L by a small tilt of the laser crystal over an angle α), there will still be a E_L field left near the crystal long-ends, which can be reduced by applying some bias to the additional contacts, allowing a further optimization of the gain.

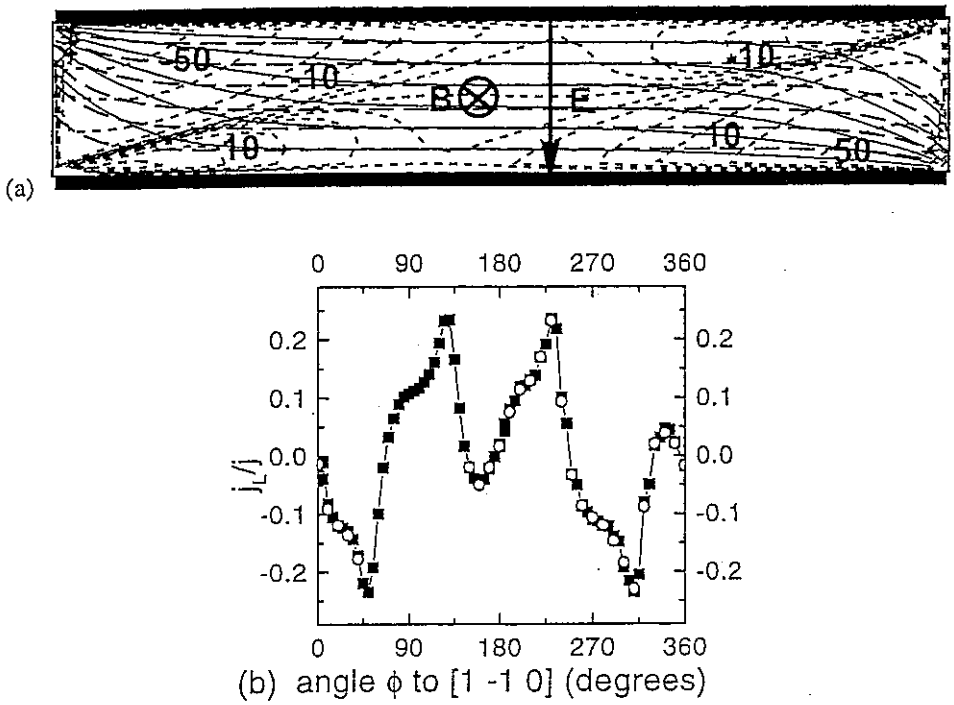

Figure 10. (a) Equipotential lines (each 100 V) in the sample cross-section perpendicular to the magnetic field for $f = 0$ (no space-charge, dash-dotted lines) and $f = 0.7$ (solid lines). The dotted lines indicate contour lines of the space charge (in units of $\varepsilon \times 10^6$ Vm^{-2}) formed for $f = 0.7$. A constant Hall-angle ($\alpha_H = 45°$) is assumed. (b) j_L/j versus the angle ϕ over which E is rotated ; $T = 20$ K, $E = 1.35$ kV/cm $\parallel [1\bar{1}0]$ (for $\phi = 0°$), $B = 1.0$ T $\parallel [112]$, $N_I = 1.3 \times 10^{14}$ cm^{-3}, $p_0 = 7 \times 10^{13}$ cm^{-3}, Brooks-Herring model with self-consistent screening.

4. CONCLUSIONS

Changing the bias to the rf modulation field of an actively mode-locked p-Ge laser yields precise control of gain modulation characteristics and allows to optimize for shortest pulses or change the time delay between two independent pulses in a laser mode locked at the second harmonic. In some cases, an external bias is required to achieve mode locking at all, to compensate deteriorating effects due to intrinsic charging of the laser crystal.

ACKNOWLEDGEMENTS

This work is supported by NSF (ECS-9531933) and AFOSR/BMDO (F49620-97-1-0434). Coauthors from IPM thank Russian Foundation for Basic Research (grants 96-02-19275, 96-02-00249 G) for support of this work.

REFERENCES

1. E. Gornik and A. A. Andronov, eds., *Opt. Quantum Electron.*, vol. 23, Chapman and Hall, London, 1991. Special Issue Far-infrared Semiconductor Lasers.
2. E. Bründermann, A. M. Linhart, H. P. Röser, O. D. Dubon, W. L. Hansen, and E. E. Haller, "Miniaturization of *p*-Ge lasers: Progress toward continuous wave operation," *Appl. Phys. Lett.* 68, pp. 1359–1361, Mar. 1996.

3. J. N. Hovenier, A. V. Muravjov, S. G. Pavlov, V. N. Shastin, R. C. Strijbos, and W. T. Wenckebach, "Active mode locking of a *p*-Ge hot hole laser," *Appl. Phys. Lett.* 71, pp. 443–445, July 1997.
4. J. N. Hovenier, T. O. Klaassen, W. T. Wenckebach, A. V. Muravjov, S. G. Pavlov, and V. N. Shastin, "Gain of the mode locked p-ge laser in the low field region," *Appl. Phys. Lett.* 72, pp. 1140–1142, Mar. 1998.
5. A. V. Muravjov, R. C. Strijbos, C. J. Fredricksen, H. Weidner, W. Trimble, A. Jamison, S. G. Pavlov, V. N. Shastin, and R. E. Peale, "Mode-locked far-infrared p-Ge laser using an offset rf electric field for gain modulation," in *Proceedings of Workshop on Radiative Processes and Dephasing in Semiconductors, February 2-4, 1998, Coeur d'Alene, Idaho*, D. Citron, ed., vol. 18 of *OSA-TOPS*, pp. 102–107, OSA, (Washington DC), 1998.
6. R. C. Strijbos, J. G. S. Lok, and W. T. Wenckebach, "A Monte Carlo simulation of mode-locked hot-hole laser operation," *J. Phys. Condens. Matter* 6, pp. 7461–7468, 1994.
7. R. C. Strijbos, J. H. Blok, J. N. Hovenier, R. N. Schouten, W. T. Wenckebach, A. V. Muravjov, S. G. Pavlov, and V. N. Shastin, "Active mode locking of a *p*-Ge light-heavy hole band laser by electrically modulating its gain: theory and experiment," in Hess *et al.*,[12] pp. 631–633.
8. R. C. Strijbos, A. V. Muravjov, J. H. Blok, J. N. Hovenier, J. G. S. Lok, S. G. Pavlov, R. N. Schouten, V. N. Shastin, and W. T. Wenckebach, "Electrically controlled gain modulation for active mode locking of far-infrared *p*-Ge hot hole lasers," in *Conference digest of 15th Int. Semiconductor Laser Conference, october 13-18, 1996, Haifa, Israel*, pp. 61–62, 1996.
9. R. C. Strijbos, *Hole transport effects in p-Ge lasers*. PhD thesis, Delft University of Technology, 1997.
10. R. C. Strijbos, S. I. Schets, and W. T. Wenckebach, "Appearance of a large 'Hall' current component parallel to B in *p*-Ge in strong crossed E and B fields," in Hess *et al.*,[12] pp. 469–471.
11. W. Sasaki and M. Shibuya, "Experimental evidence of the anisotropy of hot electrons in *n*-type germanium," *J. Phys. Soc. Jpn.* 11, pp. 1202–1203, 1956.
12. K. Hess, J.-P. Leburton, and U. Ravaioli, eds., *Hot Carriers in Semiconductors*, (New York), Proceedings of the 9th Int. Conf. on Hot Carriers in Semiconductors, July 31-August 4, 1995, Chicago, Illinois, USA, Plenum Press, 1996.